AIAA 81-2008R

Flowfield and Far Field Acoustic Amplification Properties of Heated and Unheated Jets

L. Maestrello*
NASA Langley Research Center, Hampton, Virginia
and
A. Bayliss†
Courant Institute of Mathematical Sciences, New York, New York

The interaction of an acoustic pulse with the experimentally determined mean flowfield of a spreading jet has been simulated numerically. The simulation is obtained by solving the Euler equations linearized about the spreading jet. The model shows a small, sustained oscillation long after the original pulse has passed. This remnant is seen as a continual shedding of vortices from the nozzle lip, together with the generation of acoustic ripples. The jet is also shown to act as an amplifier of sound. This amplification is traced to the stability characteristics of the jet. It is shown that some of the observed differences in the spectra of heated and unheated jets can be attributed to differences in the stability characteristics of the jets.

I. Introduction

THE purpose of this paper is to study the flowfield and far field amplification generated by the mean gradients of an axisymmetric jet. In particular, we consider the effects of velocity and temperature gradients of a jet exiting from a semi-infinite, straight nozzle. These gradients cause substantial amplification and modification of the fluctuating field in the jet. These amplifications are transmitted to the far field and strongly influence the resulting sound pattern.

The results are obtained from a numerical model that is based on the inviscid, conservation (Euler) equations. The equations are linearized about the mean state of a real, spreading jet, including a possible density (i.e., temperature) gradient. The resulting linear, hyperbolic (time-dependent) system is then forced by a pulse-like, in time, source in the continuity equation (transient mass injection). The model includes a semi-infinite, straight nozzle from which the mean flow exits.

In previous papers[1-3] the authors demonstrated that the pulse excites large-scale structures (instability waves) that are supported by the linearly unstable mean state. These structures are associated with an overall increase in the far field acoustic power, a result consistent with experimental measurements.[1,4] In this paper, we study the directionality of the instability generated sound. Several far field peaks are shown to occur in the spectra at different angles. These peaks are qualitatively explained as being generated by several different large-scale structures. In particular, changes in the far field spectra due to the heating are shown to correlate with changes in the growth rates of the unstable mean flow brought about by the heating.

We also study the long time behavior of the fluctuations. A small, self-sustained oscillation is shown to exist long after the original pulse has passed. This remnant is associated with a continual shedding of vortices from the nozzle lip. The results show that the behavior of the jet after the pulse has passed is very similar to the behavior of unforced, real jets excited by the natural sources. This is very surprising, given the linearity of the model.

Presented as Paper 81-2008 at the AIAA 7th Aeroacoustics Conference, Palo Alto, Calif., Oct. 5-7, 1981; submitted Oct. 16, 1981; revision received March 15, 1982. This paper is declared a work of the U.S. Government and therefore is in the public domain.

*Research Scientist. Member AIAA.
†Associate Professor. Member AIAA.

The validity of the model depends on 1) justification of the linearization of the fluctuations relative to the mean state, 2) appropriate choice of the mean state to use in the linearized operator, and 3) correct treatment of the fluctuating field at the nozzle lip.

Points 1 and 2 are, of course, related. The concept of linearization has a long history in acoustics. In particular, Phillips[5] and Lilley[6] have developed acoustic models based on linearizing about some mean flow. These flows were usually parallel (i.e., no axial dependence) and were thus, automatically, solutions of the unforced Euler equations. In fact, realistic instability waves are not properly modeled[7,8] in a nonspreading jet. The waves will grow indefinitely rather than exhibit the growth and decay due to the jet spreading. It is, therefore, more realistic to linearize about a spreading jet. Our choice is a spreading model based on measurements of one of the authors.[9] This data was obtained for the mean flow of a turbulent jet that was found to be relatively insensitive to the Reynold's number. This mean profile will not, of course, be a solution to the unforced Euler equations. However, the appearance of the mean flow as coefficients of the resulting linearized differential operator permits us to make small changes in the mean state without greatly altering the solution (i.e., the problem is well-posed with respect to changes in the coefficients).

In our model we study the response of this mean flow to a given source. The model generates the complete, time-dependent solution which includes both acoustic and nonacoustic components, each evolving on its own time scale. Crighton[10] has argued that the time scales associated with the sound generated by the turbulent sources are not large compared with the time scale on which the flow acts as a mean flow. This is particularly true when high-frequency turbulent fluctuations are considered. The effect of these fluctuations, however, is essentially confined to high frequencies which are not, in any event, resolved by the numerical simulation. The phenomena discussed here are essentially confined to the low- and middle-frequency range which is not strongly influenced by high-frequency turbulent fluctuations in the jet.

The proper treatment of the nozzle lip is of great importance in simulating the physics of the response of the jet to the source. Vorticity can be generated through two mechanisms: 1) direct interaction of the fluctuating field with the nozzle lip, and 2) vorticity associated with instability waves convecting through the unstable mean profile.

Point 2 is not outwardly related to the nozzle. However, we can make the obvious statement that the jet had to come from somewhere and thus the nozzle can be regarded as generating the instability in the problem. Point 1 is more subtle and is very much related to the Kutta condition at the nozzle lip. The usual Kutta condition is designed to deal with steady flow and is not relevant here. Time-dependent versions of the Kutta condition have been proposed[11] but we will simply take as the Kutta condition the condition that the fluctuating velocities and pressure be finite at the nozzle lip (see Crighton[12]).

In model problems, the solution satisfying the radiation condition at infinity is not finite at the nozzle lip. In order to make it finite, an appropriate multiple of an unstable eigenfunction must be added to the solution. This results in instability waves and vortices downstream of the nozzle lip. In our model the nozzle is assumed to have a finite thickness and there is, thus, an effective finite thickness of the shear layer at the nozzle exit. It is not clear whether any special boundary condition is required at the nozzle lip. The treatment of the nozzle lip is described in detail in Sec. II and does insure that the solution is finite there.

The numerical results show a residual acoustic remnant together with a continual shedding of vorticity from the nozzle lip. We speculate that this is due to a linear acoustic coupling. These shed vortices generate a sound field, which in turn requires more vortices to be shed in order to force finite fluctuations in the vicinity of the nozzle lip. A more accurate simulation of this phenomenon will require more resolution near the nozzle lip and probably nonlinear interactions between the shed vortices.

The concept of sound generated from large-scale structures, as well as its amplification, is treated as a linear effect. The properties of the jet as an amplifier depend crucially on the stability characteristics of the mean flow. The results presented in Ref. 3 and in the present paper clearly demonstrate that stability differences induced by a temperature profile in the mean flow will explain, at least partially, the observed differences between the far field acoustic spectra of heated and unheated jets. In particular, the growth rates for heated jets are shifted into lower frequencies and are reduced by heating. The computed far field spectrum exhibits similar properties, which is consistent with experimental measurements.[13,14]

The concept of the jet as an amplifier (albeit only above a threshold excitation level) is supported by experimental data in Ref. 1 where the jet is excited downstream of the nozzle. It is perhaps also supported by the broadband amplification observed, for example, in Ref. 4 where the excitation is upstream of the nozzle. Usual methods of exciting the jet upstream of the nozzle cause an attenuation of the sound at the exciting frequency.[4,12] This has also been studied analytically by Howe.[15] In our model, the jet is excited downstream of the nozzle and, in fact, the boundary conditions are designed to simulate a flux of energy up the pipe only.

In Sec. II, we discuss the numerical model. Results are presented in Sec. III. In Sec. IV, we present a summary of our conclusions.

II. Numerical Model

The numerical model consists of the inviscid, conservation (Euler) equations linearized about a mean state corresponding to experimental data for a round jet. The jet is excited by transient mass injection, simulated by a source (units density/time) in the continuity equation. The source is assumed to have a small amplitude which we denote by ϵ ($\epsilon \ll 1$). Therefore, the actual source is ϵm where m is 0(1) and has units density/time. The total solution is written as $(\rho_0, P_0, U_0, V_0) + \epsilon(\rho', p', u', v')$ where ρ is the density, p the pressure, and u and v the axial and radial velocities, respectively. For simplicity we assume a constant mean pressure (i.e., $P_0 = P_\infty$) where P_∞ denotes the ambient pressure. Throughout this paper, the subscript 0 will refer to the mean state while the subscript ∞ will refer to the ambient state.

This expression is substituted into the full, nonlinear Euler equations and only first-order terms in ϵ are kept. If we let r and z denote the radial and axial coordinates, respectively, and drop the primes for simplicity, we obtain the following system of equations.

Mass

$$\frac{\partial \rho}{\partial t} + \frac{\partial}{\partial z}(\rho_0 u + U_0 \rho) + \frac{\partial}{\partial r}(\rho_0 v + V_0 \rho) + \frac{\rho_0 v + V_0 \rho}{r} = m \tag{1a}$$

Energy

$$\frac{\partial p}{\partial t} + \frac{\partial}{\partial z}(U_0 p + \gamma P_0 u) + \frac{\partial}{\partial r}(V_0 p + \gamma P_0 v) + \frac{\gamma P_0 v + V_0 p}{r} = c_0^2 m \tag{1b}$$

Axial momentum

$$\frac{\partial u}{\partial t} + \frac{\partial}{\partial z}\left(U_0 u + \frac{p}{\rho_0}\right) + \frac{\partial}{\partial r}(V_0 u) = -\frac{p}{\rho_0^2}\frac{\partial \rho_0}{\partial z} - \frac{v \partial U_0}{\partial r} + \frac{u \partial V_0}{\partial r} \tag{1c}$$

Normal momentum

$$\frac{\partial v}{\partial t} + \frac{\partial}{\partial z}(U_0 v) + \frac{\partial}{\partial r}\left(V_0 v + \frac{p}{\rho_0}\right) = -\frac{p}{\rho_0^2}\frac{\partial \rho_0}{\partial r} + \frac{v \partial U_0}{\partial z} - \frac{u \partial V_0}{\partial z} \tag{1d}$$

(Here γ is the ratio of the specific heats.) Observe that ϵ disappears in the final system. Its role is merely as a bookkeeping parameter to assist in the linearization.

The mean velocities U_0 and V_0 were taken from experimental data for a jet of Reynold's number 8×10^5 and diameter 5.08 cm. The mean velocity V_0 is very small and the terms involving V_0 and its derivatives have practically no effect on the solution. The data presented here were obtained with these terms omitted from the simulation. No other terms are omitted from the simulation although $\partial U_0/\partial z$ is of the same order as $\partial V_0/\partial r$. It also has practically no effect on the solution.

Temperature variations are taken into account by an expression due to Crocco (see Michalke and Michel[16])

$$\frac{T_0}{T_\infty} = 1 + \left(\frac{T_j}{T_\infty} - 1\right)\left(\frac{U_0}{U_j}\right) + \left(\frac{\gamma - 1}{2}\right) M_j^2 \frac{U_0}{U_j}\left(1 - \frac{U_0}{U_j}\right)$$

Here, T_j and M_j are the jet exit temperature and Mach number, respectively. (The subscript j will always denote a quantity at the jet exit.) For our runs with the heated jet, we took $T_j/T_\infty = 3.0$.

The source is modeled by the functional form

$$m(t,z,r) = \frac{\rho_\infty c_\infty}{D} \exp[-(at^2 + b/t^2)]\,\delta[r^2 + (z - z_s)^2]$$

where D is the nozzle diameter and c_∞ the ambient sound speed. The constants a and b (units time^{-2} and time^2, respectively) are chosen so that the spectrum of the forcing pulse peaks at roughly 1100 Hz if the units of time are seconds. Based on a diameter D of 5.08 cm and a speed of sound $c_\infty = 350$ m/s this corresponds to a Helmholtz number

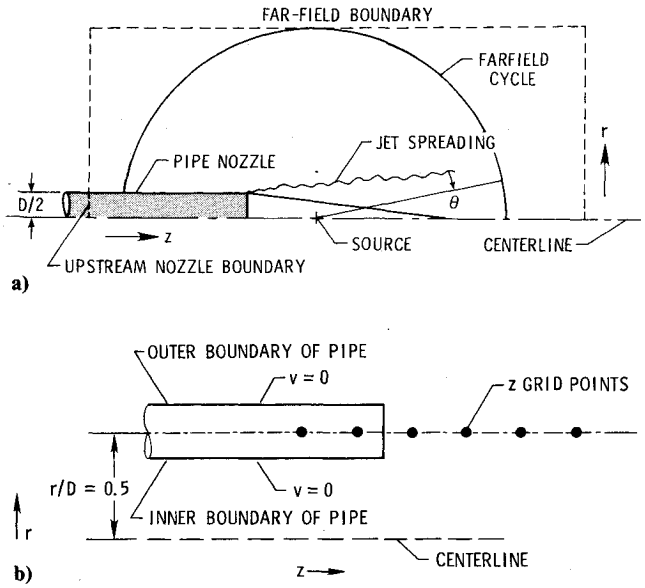

Fig. 1 a) Computational domain. b) Grid points about the nozzle lip.

fD/c_∞ of about 0.16. The source location z_s is $1.15D$ downstream of the nozzle. The delta function is approximation by a Gaussian

$$4\pi\left(\frac{40}{\pi}\right)^{3/2}\exp\left\{-40\left[\left(\frac{r}{D}\right)^2+\left(\frac{z-z_s}{D}\right)^2\right]\right\}$$

Increasing the sharpness of the Gaussian does not change the solution very much. The initial conditions are zero so that initially the state is quiescent. Severe coordinate stretching is used in the vicinity of the flow.

Observe that the perturbations p, u, and v do not depend on the perturbed density but ρ depends on p, u, and v. This is similar to the case of the unheated jet. However, it will not be the case that $p=c_\infty^2\rho$, as is true in the unheated jet. This is because ρ_0 is variable while P_0 is constant. The system is solved in the cylindrical region shown in Fig. 1a. Far field measurements are computed on a circle centered at the source and as a function of the polar angle θ indicated in Fig. 1a. The numerical scheme is a 2-4 (second order in time, fourth order in space) version of the MacCormack scheme[17] and is described in great detail in Ref. 1. Radiation boundary conditions are prescribed at the far field boundaries. These conditions are discussed in Ref. 1 and studied extensively in Ref. 18. Computations are also carried out inside the nozzle. At the upstream boundary, a boundary condition is imposed which ensures that waves travel only up the nozzle. This condition is described in Ref. 1.

Since the nozzle lip is important to the resulting sound field, we will describe how we deal with it. The nozzle is considered to have finite thickness, with upper and lower faces determined by the grid points $\{r_j\}$ such that $\{r_j/D\}$ are as close as possible to 0.5. The nozzle is treated as a solid wall with the condition $v=0$ imposed on the inside and the outside. One-sided differences (described in Ref. 1) are used whenever the finite-difference approximation requires grid points which are not available due to the wall (see Fig. 1b). The nozzle is assumed to end midway between two z grid points and z differences are computed directly across the nozzle lip. Numerical investigation confirms that the velocities remain bounded near the lip.

III. Results

In order to set a frame of reference, we first describe the fluctuating field in the vicinity of the flow. In Figs. 2 and 3, the fluctuating pressure $p(t,z,r)$ is plotted as a function of t

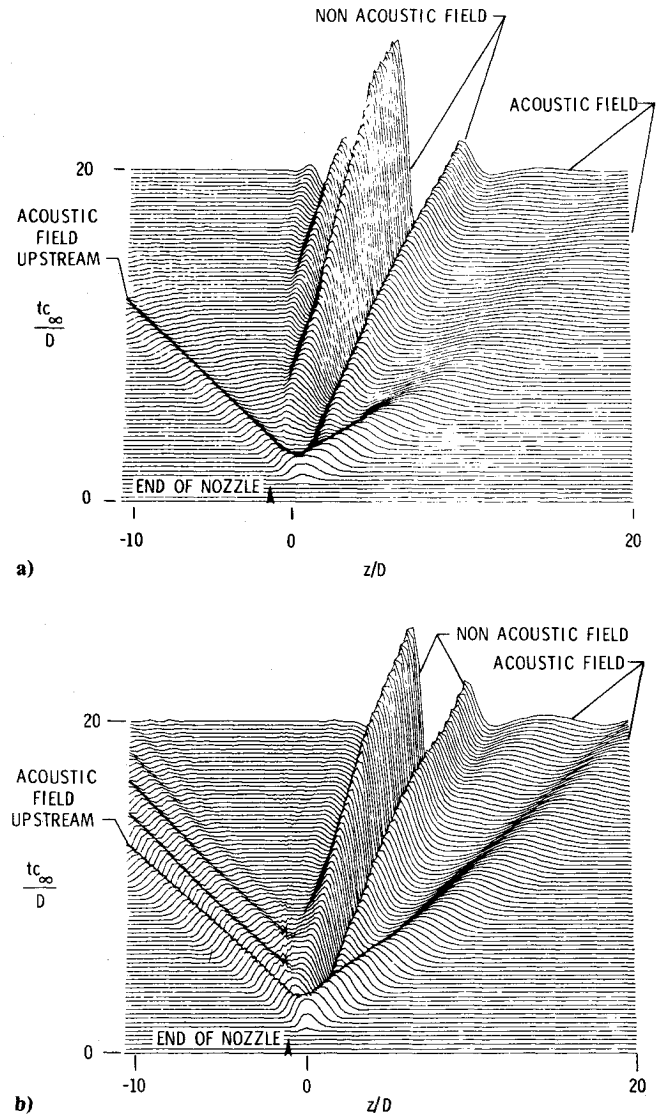

Fig. 2 Three-dimensional plot of fluctuating pressure; a) heated jet: $T_j/T_\infty=3.0$, $U_j/c_\infty=0.66$, and $r/D=0.735$; and b) unheated jet: $T_j/T_\infty=1.0$, $U_j/c_\infty=0.66$, and $r/D=0.735$.

and z at a fixed r location ($r/D=0.735$). The results are presented for both heated and unheated jets and for $M_j=0.66$ and $M=0.85$. The data are scaled by the distance from the source d in order to de-emphasize the $0(1/d)$ acoustic decay. The ambient sound speed c_∞ is normalized to unity in the figures.

An acoustic pulse, propagating with speed close to unity, can be observed. Two large pulses follow the acoustic pulse. These pulses are nonacoustic and, by close examination of this and other figures (not shown), we infer that their speed of propagation is approximately $0.7U_j$ for both heated and unheated jets. These pulses are instability waves excited by the source. The properties of these waves are very similar to the large scale structures observed by Crow and Champagne[19] and others.

It can also be seen that the leading wave (downstream) is generated somewhat downstream of the source, probably by the pulse intersecting the jet shear layer. The trailing wave (upstream) clearly is generated at the axial position of the nozzle lip. The waves in the heated jet are somewhat broader, reflecting a lower frequency content. An additional, smaller amplitude wave appears to be generated at the nozzle lip in the heated jet.

A series of acoustic ripples can be seen propagating around but primarily upstream of the nozzle. They are particularly

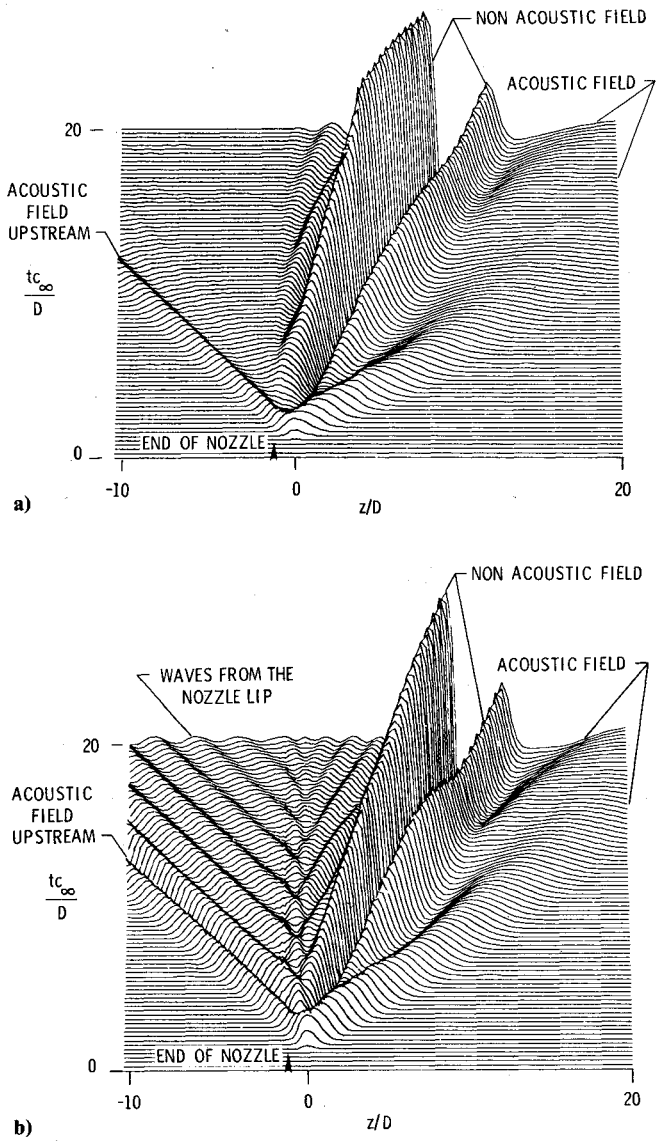

Fig. 3 Three-dimensional plot of fluctuating pressure; a) heated jet: $T_j/T_\infty = 3.0$, $U_j/c_\infty = 0.85$, and $r/D = 0.735$; and b) unheated jet: $T_j/T_\infty = 1.0$, $U_j/c_\infty = 0.85$, and $r/D = 0.735$.

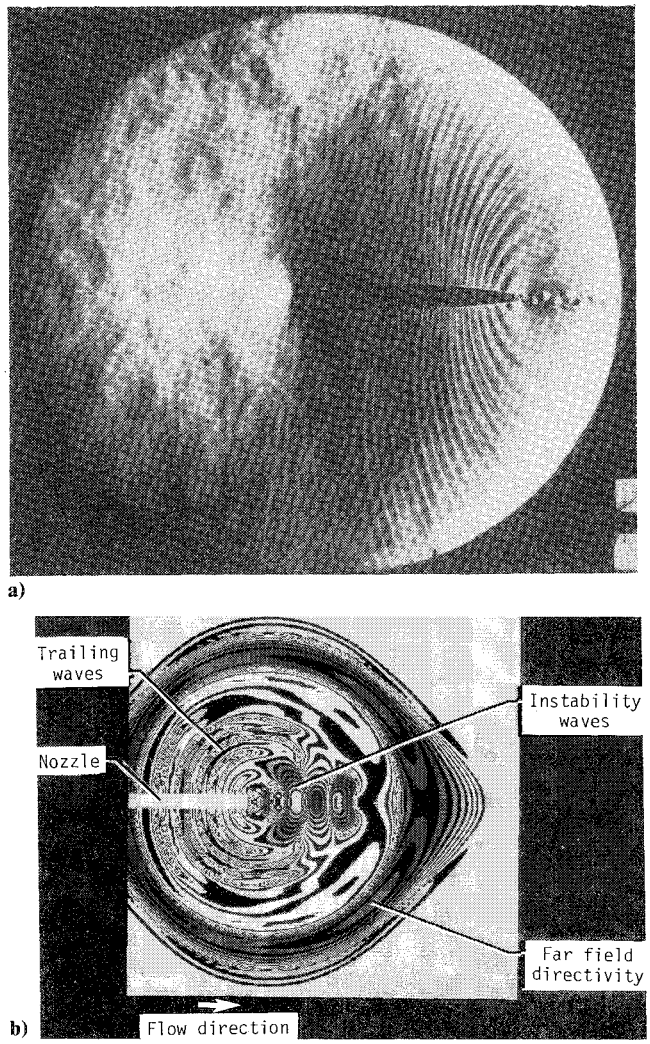

Fig. 4 a) Schlieren photograph of the trailing waves of an airfoil (experiment conducted at NASA Langley years ago). b) Contours of fluctuating pressure propagating upstream and downstream of the nozzle lip.

evident in Fig. 3b (unheated jet, $M_j = 0.85$). These ripples are much weaker in the heated jet (Fig. 3a). A possible reason for this is the reduced mean density at the nozzle. They do not contribute much to the total far field power. These ripples are very similar to the sound pattern generated at the trailing edge of an airfoil with a slightly blunt edge. This phenomenon is illustrated in Figs. 4a and 4b where a schlieren photograph of the wake of an airfoil is compared with a visualization of the fluctuating pressure around the nozzle lip. Figure 4b manifests a similar behavior to Fig. 4a.

We believe that these highly directional (upstream) acoustic ripples are not associated with the instability of the mean flow nor of the acoustic remnant generated by the vortex shedding and described subsequently. This is primarily a diffraction effect which would be obtained even from solutions based on the convective wave equation where instability waves do not exist.

In order to demonstrate the shedding of vorticity, which is generated by the attempt of the solution to adjust to the boundedness of the fluctuations at the nozzle lip, we plot in Fig. 5a the fluctuating vorticity in the unheated jet at $tc_\infty/D = 10.3$. The figure illustrates two large intense vortices. These vortices are associated with the instability waves in the flow. (They convect downstream at roughly the same velocity $\sim 0.7U_j$.) In Fig. 5b the fluctuating vorticity is plotted for a sequence of later times ($tc_\infty/D \sim 30$). The figure clearly illustrates the continual shedding of vortices long after the triggering pulse has decayed. These vortices are generated at the nozzle lip and are a consequence of the linear acoustic coupling discussed earlier. Very similar results are obtained in the heated jet.

The shedding frequency of the vortices from the nozzle lip can be estimated from the figure. The shedding rate f normalized by the nozzle thickness $\Delta(\sim 0.11D)$ satisfies $f\Delta/U_j = 0.044$. The spectrum of the acoustic remnant in the far field peaks at a frequency very close to this. This can be seen in Fig. 6. This data certainly indicates that the far field (acoustic) remnant is sound, generated by the rate of vortex shedding from the nozzle lip. This is one of the mechanisms of sound generation in a real unforced jet.

Reference 20, as well as others, has shown that vortices shed in a jet at a frequency f corresponding to $f\bar{\theta}/U_j = 0.0116$ where $\bar{\theta}$ is the momentum thickness at the nozzle exit. In this jet $\bar{\theta}$ is much smaller than Δ, thus accounting for the larger shedding rate. Reducing Δ to $0.08D$ from $0.11D$ reduced the nondimensional shedding rate $f\Delta/U_j$ to 0.036 from 0.044, thus apparently converging to the experimentally determined rate for an infinitely thin nozzle lip. At the present time it is not possible for our code to resolve the frequencies observed experimentally.

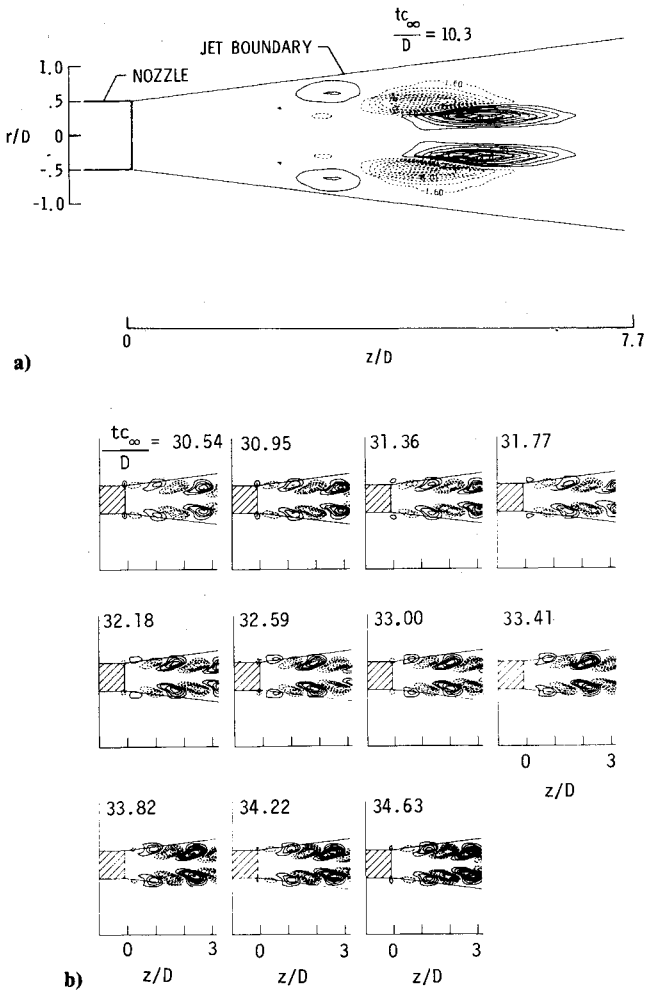

Fig. 5 a) Vorticity for unheated jet; dashed curves denote regions of clockwise rotation; $U_j/c_\infty = 0.66$ and $T_j/T_\infty = 1.0$. b) Sequence of vorticity contours corresponding to one period of the vortex shedding; dashed curves denote regions of clockwise rotation; $U_j/c_\infty = 0.66$ and $T_j/T_\infty = 1.0$.

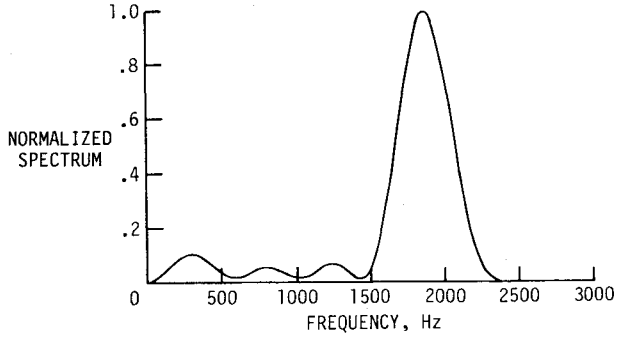

Fig. 6 Far field spectra of sound generated by the shedding rate of vorticity at the nozzle lip, $T_j/T_\infty = 1.0$ and $U_j/c_\infty = 0.66$.

In real jets the far field sound spectrum is considerably broader than that shown in Fig. 6. This is because of vortex pairing further downstream as well as other nonlinear and three-dimensional effects. These effects are not included in the numerical simulation. However, the results clearly demonstrate the generation of sound from vorticity generation at the nozzle lip. We stress that these results were obtained in a linear program and that the excitation mechanism has long since decayed to zero.

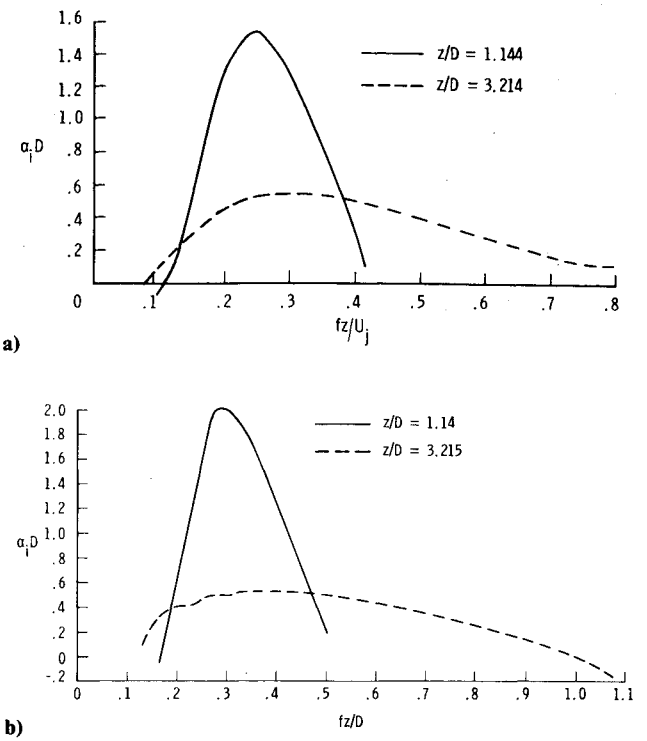

Fig. 7 Growth rates for jets, $U_j/c_\infty = 0.66$; a) heated jet, $T_j/T_\infty = 3.0$ and b) unheated jet.

The behavior illustrated in Figs. 5a and 5b is very similar in both the heated and unheated jets. This leads again to the conclusion that this behavior primarily is due to the geometry around the nozzle lip. The temperature gradients are more important in influencing properties that depend directly on the stability of the mean profile.

In order to characterize the effects that temperature gradients have on the stability properties of the flow, we first consider the growth rates of exponentially growing instability waves. For parallel flow (no z dependence) it is customary to analyze the behavior of time harmonic solutions. In fact, solutions to the Euler equations of the form

$$\begin{Bmatrix} \rho(t,z,r) \\ p(t,z,r) \\ u(t,z,r) \\ v(t,z,r) \end{Bmatrix} = e^{i(\omega t - \alpha z)} \begin{Bmatrix} \hat{\rho}(r) \\ \hat{p}(r) \\ \hat{u}(r) \\ \hat{v}(r) \end{Bmatrix} \tag{2}$$

exist for any value of ω. The spatial growth rate $\alpha(\omega)$ and the functions $\hat{\rho}(r)$ etc., are obtained by finding the eigenvalues and eigenfunctions of the Orr-Summerfeld equations given boundedness conditions as $r \to \infty$. The growth (or decay) of solutions of the form of Eq. (2) is determined by the imaginary part of α,(α_i).

In a spreading jet, solutions of the form of Eq. (2) no longer exist, because of the z dependence of the mean flow. In this case we can find local approximations to the growth rate by the following procedure.

The numerical data for any particular quantity, say p, is known for a discrete time grid t_j ($=j\Delta t$). Thus at any fixed spatial location we have a sequence $p(t_j,z,r)$. These data can then be numerically Fourier transformed to yield a sequence $\hat{p}(\omega_j,z,r)$. If the r position is fixed, then from Eq. (2) we can see that the growth rate α_i can be obtained from the formula

$$\alpha_i(\omega_j) = \frac{\mathrm{d}}{\mathrm{d}z} \log |\hat{p}(\omega_j,z,r)|$$

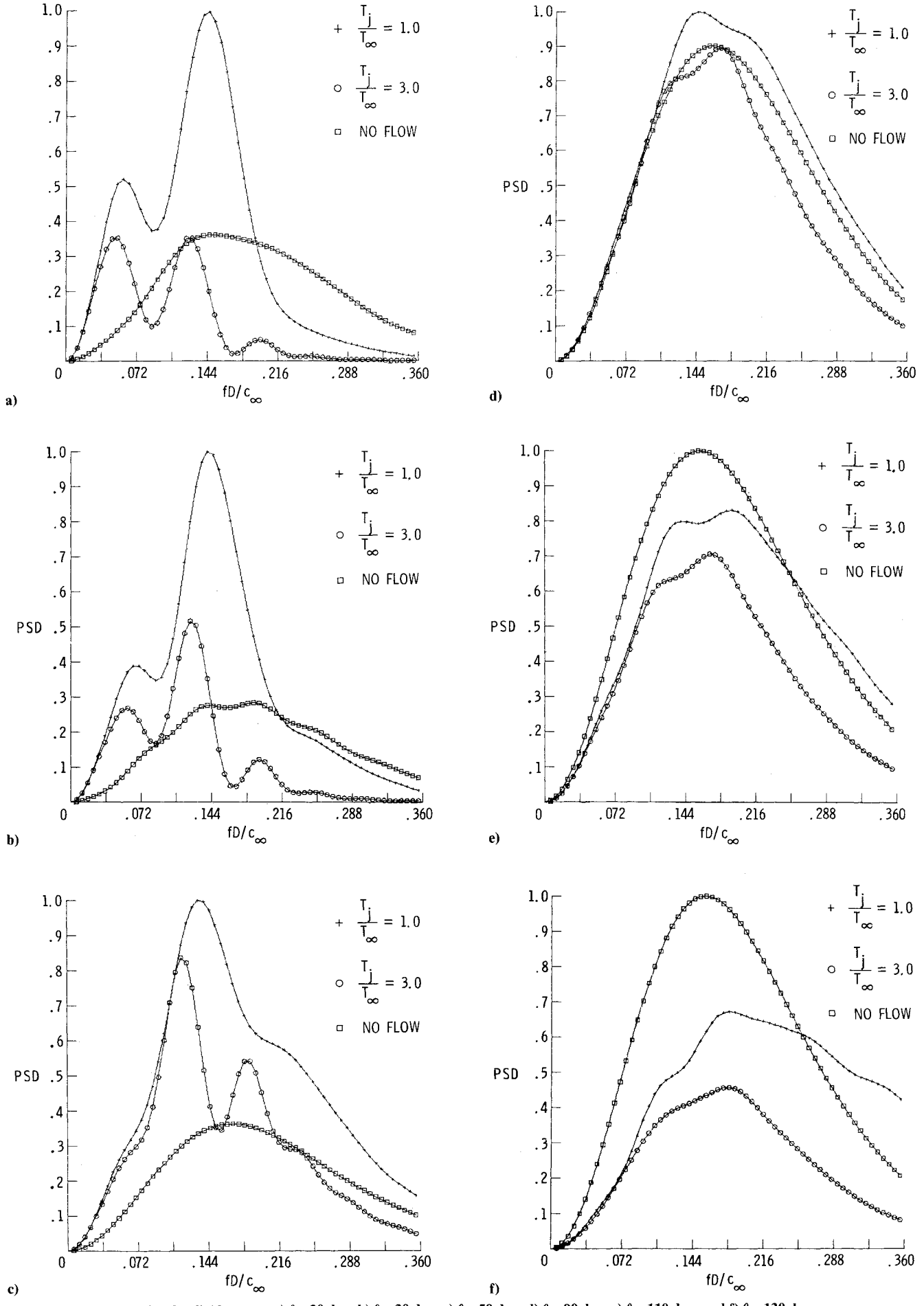

Fig. 8 Far field spectra a) $\theta = 20$ deg, b) $\theta = 30$ deg, c) $\theta = 50$ deg, d) $\theta = 90$ deg, e) $\theta = 110$ deg, and f) $\theta = 130$ deg.

The expression Eq. (2) can now be approximated numerically by using a centered difference approximation to the derivative.

This procedure must be applied with care as it assumes that the solution is composed entirely of instability waves. However, it is apparent from Figs. 2 and 3 that this is a valid approximation near the source. The computed nondimensional growth rates $\alpha_i D$ are plotted in Figs. 7a and 7b vs longitudinal Strouhal number (fz/U_j) for both heated and unheated jets. These results are for a constant velocity jet and the Mach number, based on the ambient sound speed, is 0.66. [The data are for the axial velocity u, since the growth rates are different for all four quantities in Eq. (2) due to the spread of the jet. The figures are qualitatively similar for the fluctuating pressure.]

The data established two important features.

1) The growth rates are reduced by heating, particularly for locations close to the jet.

2) Frequencies of significant growth rates tend to be shifted downward due to the heating. These characteristics will directly influence the far field sound pattern.

The stabilizing effects of temperature gradients for constant velocity jets are consistent with the analyses of Gill and Drazin[21] and Fung.[22] Michalke[23] studied numerically the growth rates of a very low-speed parallel flow with temperature gradients. He found that at a constant exit Mach number heating tended to destabilize the flow. Since a constant Mach number implies an increased exit velocity when the jet is heated this is not inconsistent with the results presented here.

In order to analyze the far field data, we Fourier transform the fluctuating pressure on a sphere of radius $47D$ and plot the power spectral density (PSD) as a function of frequency at various angles. The data are taken by truncating the pulse solution at a large enough time so that the residual solution is negligible compared with the acoustic pulse. We have experimented by taking data over a larger time interval. This has virtually no effect on the far field data.

In Figs. 8a-f these data are shown for the heated and unheated jets and also for the pulse without flow. The data are given for the far field angles $\theta = 20$, 30, 50, 90, 110, and 140 deg and are normalized so that the peak observations may be made from these data.

The solution without any flow represents closely a nearly omnidirectional source with a peak Helmholtz number (fD/c_∞) of 0.16. Based on a diameter D of 5.08 cm and an ambient sound speed of 350 m/s this corresponds to a frequency of about 1100 cycles/s. The deviation from omnidirectionality is very small and is probably due to the approximation of the delta function by a Gaussian.

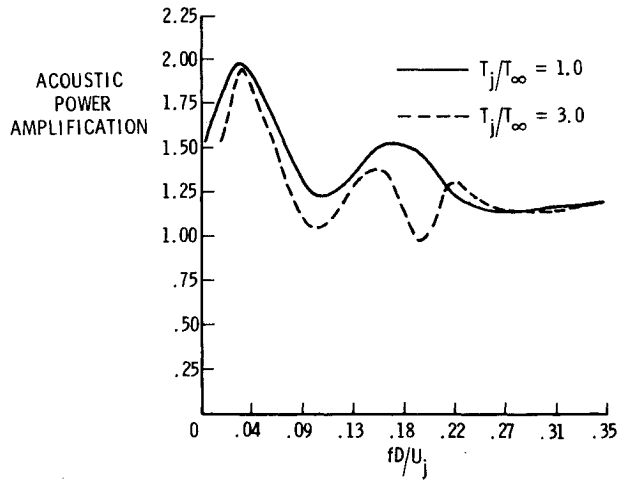

Fig. 9 Total acoustic power amplification due to the flow.

In the solutions with flow, other peaks appear. A low-frequency peak at around fD/c_∞ of 0.043 is present up to 30 deg. A higher peak at around fD/c_∞ of 0.11 (lower for the heated jet) is visible up to 90 deg where all solutions are roughly similar. For angles up to 90 deg a further peak appears for the heated jet. Beyond 90 deg no additional peaks appear. This indicates that the instability generated sound is radiated primarily downstream.

In the absence of any additional sound generation, i.e., due to instability, we would expect no additional peaks and that the signal peak would shift in frequency with far field angle, due to refraction (i.e., the preferential bending of higher frequencies away from the jet axis). It is, in fact, possible to observe this numerically by omitting the mean shear terms from the system of Eqs. (1) (i.e., the terms depending on the derivatives of U_0). Instability waves cannot exist in this case. We have verified this numerically, although it easily can be seen that in this case the system of Eqs. (1) reduces to a convective wave equation which cannot support instability waves (assuming parallel flow).

Upon carrying out this purely numerical experiment, excluding the mean shear terms, no near field instability waves were seen, in contrast to the results shown in Figs. 2 and 3. In addition, no other peaks appeared in the far field spectra, in contrast to the results shown in Figs. 8a-f. Of course, the resulting equations are no longer the linearized Euler equations. However, this does show that these shear terms (identified by Ribner, and others, as the shear noise terms[24]) act both to destabilize the flow and to generate the additional spectral peaks. The primarily downstream radiation produced from the instability waves is consistent with predictions for directionality of the shear noise terms (see, for example, Ribner[24,25]). It should be pointed out that the angles are taken with origin at the source location rather than at the nozzle exit. However, due to the nearness of the source to the nozzle exit ($1.15D$) this effect is negligible in comparing with the directivity patterns of Ref. 24.

It is also clear from the figures that the peaks for the heated jet are shifted downward in frequency and reduced in amplitude from the unheated jet. This behavior is very similar to the behavior of the growth rates shown in Figs. 7a and 7b.

The conclusion we draw from these observations is that these peaks represent sound generated from the instability waves seen in Figs. 2 and 3. The low-frequency peak, beamed at low angles to the jet axis, has its source where the peak frequencies are lower (scaling as fz/U_j). The mid-frequency peak is generated from the trailing instability wave generated at (or very close to) the nozzle lip. This frequency is sufficiently close to the peak of the forcing pulse that no separate peak is visible (although a slight blip indicating the forcing pulse is visible in some of these figures). Based on the preceding, we suggest that the third peak in the heated jet is due to the splitting of the trailing instability wave seen in Fig. 2a.

Figure 9 is intended to further illustrate the characteristics of the jet as an amplifier. It is a plot of the ratio of the total far field power/unit frequency of the simulations with and without flow. The figure clearly illustrates the downward shift in the heated jet.

The following summarizes these conclusions.

1) Heating causes a shift of the far field spectra toward lower frequencies.

2) Heating causes a reduction in the amplification of sound due to the flow.

3) These properties, consistent with experimental observations,[13,14] are at least partly attributable to the changed stability characteristics of a heated jet.

IV. Conclusion

We have numerically simulated the interaction of an acoustic pulse with a flow exiting from a semi-infinite, straight nozzle. The simulation is obtained by linearizing the

Euler equations about a given mean profile. The nozzle lip is treated numerically in a manner that assumes bounded solutions, although basically the solution is allowed to seek its own behavior at the nozzle lip.

The results show a small self-sustained oscillation (remnant) after the initial pulse has moved away. This remnant has strong similarities with the behavior of real jets excited by the natural sources. This indicates the importance of the nozzle lip in causing this behavior.

In addition, the properties of a jet flow as an amplifier of sound have been studied. This amplification has been shown to be due to the stability characteristics of the flow. The heating of the jet has been shown to reduce the peak amplification and cause a shift toward lower frequencies. This provides an explanation in terms of stability characteristics of experimentally observed phenomena.

Acknowledgments

This work was partially supported under NASA Contracts NAS1-14472 and NAS1-15810 while the second author was in residence at the Institute for Computer Applications in Science and Engineering, NASA Langley Research Center, Hampton, Va. Additional support for the second author was provided by Air Force Contract AFOSR-81-0020, and the Department of Energy Contract No. DE-AC02-76ER03077. The authors would like to gratefully acknowledge many helpful suggestions made by Prof. H.S. Ribner during the course of review of this manuscript. The authors would also like to thank Mr. Stan Lamkin for assistance in obtaining the numerical results presented here.

References

[1] Maestrello, L., Bayliss, A., and Turkel, E., "On the Interaction of a Sound Pulse with the Shear Layer of an Axisymmetric Jet," *Journal of Sound and Vibration,* Vol. 74, 1981, pp. 281-301.

[2] Bayliss, A. and Maestrello, L., "Simulation of Instabilities and Sound Radiation in a Jet," *AIAA Journal*, Vol. 19, July 1981, pp. 835-841.

[3] Bayliss, A. and Maestrello, L., "The Interaction of a Sound Pulse with the Shear Layer of an Axisymmetric Jet, II Heated Jets," to appear in the *Journal of Sound and Vibration.*

[4] Bechert, D.W. and Pfizemmaier, E., "On the Amplification of Broad Band Jet Noise by Pure Tone Excitation," *Journal of Sound and Vibration*, Vol. 43, Dec. 1975, pp. 581-587.

[5] Phillips, O.M., "On the Sound Generated by Turbulent Shear Layers," *Journal of Fluid Mechanics*, Vol. 9, Pt. 1, Sept. 1970, pp. 657-670.

[6] Lilley, G.M., "Theory of Turbulence Generated Jet Noise: Generation of Sound in a Mixing Region," AFAPL-TR-72-53, Vol. IV, 1972.

[7] Michalke, A., "Sound Generation by Amplified Disturbances in Free Shear Layers," German Air and Space Travel Research Rept. 69-90, 1969.

[8] Tam, C.K. and Morris, P.J., "The Radiation of Sound by the Instability of a Compressible Plane Turbulent Shear Layer," *Journal of Fluid Mechanics*, Vol. 98, Pt. 2, May 1980, pp. 349-381.

[9] Maestrello, L., "Acoustic Energy Flow from Subsonic Jets and Their Mean and Turbulent Flow Structure," Ph.D. Thesis, University Southampton, 1975.

[10] Crighton, D.G., "Why do the Acoustics and Dynamics of a Hypothetical Mean Flow Bear on the Issue of Sound Generation by Turbulence?" *Symposium on Mechanics of Sound Generation in Flow*, edited by E.A. Müller, Aug. 1979, pp. 1-5.

[11] Stewartson, K., "On the Flow Near the Trailing Edge of a Flat Plate II," *Mathematika*, Vol. 16, 1969, pp. 106-121.

[12] Crighton, D.G., "Acoustics as a Branch of Fluid Mechanics," *Journal of Fluid Mechanics*, Vol. 106, May 1981, pp. 261-298.

[13] Hoch, R.G., Duponchell, J.P., Cocking, B.J., and Bryce, W.D., "Study of Influence of Density in Jet Noise," *Journal of Sound and Vibration,* Vol. 28, June 1973, pp. 648-668.

[14] Lassiter, L.W. and Hubbard, H.H., "Some Results of Experiments Relating to the Generation of Noise in Jets," *Journal of the Acoustical Society of America*, Vol. 27, No. 3, May 1955, pp. 431-437.

[15] Howe, M., "Attenuation of Sound in a Low Mach Number Nozzle Flow," *Journal of Fluid Mechanics*, Vol. 91, Pt. 2, 1979, pp. 209-229.

[16] Michalke, A. and Michel, U., "Prediction of Jet Noise in Flight from Static Tests," *Journal of Sound and Vibration*, Vol. 67, Dec., 1979, pp. 341-367.

[17] Gottlieb, D. and Turkel, E., "Dissipative Two-Four Methods for Time-Dependent Problems," *Mathematics of Computation*, Vol. 30, Oct. 1976, pp. 703-723.

[18] Bayliss, A. and Turkel, E., "Radiation Boundary Conditions for Wave Like Equations," *Communications on Pure and Applied Mathematics*, Vol. 23, Nov. 1980, pp. 707-725.

[19] Crow, S.C. and Champagne, F.H., "Orderly Structure in Jet Turbulence," *Journal of Fluid Mechanics*, Vol. 48, Pt. 3, April 1971, pp. 547-591.

[20] Ho, C.-M. and Huang, L.-S., "Subharmonics and Vortex Merging in Mixing Layers," to appear in the *Journal of Fluid Mechanics*, Vol. 119, June 1982, pp. 443-473.

[21] Gill, A.E. and Drazin, P.G., "Note on Instability of Compressible Jets and Wakes to Long-Wave Disturbances," *Journal of Fluid Mechanics*, Vol. 22, June 1965, p. 415.

[22] Fung, Y.T., "Unstable Waves of Axisymmetric Jet Flows with Density," unpublished manuscript.

[23] Michalke, A., "Instabilität eines Compressiblen runden Freistrahls unter Berucksichtigung des Einflusses der Strahlgrenzschichtdicke," *Zeitschrift für Flugwissenschaften*, Vol. 19, 1971, pp. 319-328.

[24] Ribner, H.S., "On the Role of the Shear Term in Jet Noise," *Journal of Sound and Vibration*, Vol. 52, May 1977, pp. 121-132.

[25] Ribner, H.S., "Dryden Lecture: Perspectives on Jet Noise," AIAA Paper 81-0428, Jan. 1981; also *AIAA Journal*, Vol. 19, Dec. 1981, pp. 1513-1526.